# Determination of the Boltzmann Constant by Means of Precision Measurements of $H_2{}^{18}O$ Line Shapes at 1.39 $\mu$m

L. Moretti,[1] A. Castrillo,[1] E. Fasci,[1] M. D. De Vizia,[1] G. Casa,[1] G. Galzerano,[2] A. Merlone,[3] P. Laporta,[2] and L. Gianfrani[1,*]

[1]*Dipartimento di Matematica e Fisica, Seconda Università di Napoli, I-81100 Caserta, Italy*
[2]*Istituto di Fotonica e Nanotecnologie–CNR and Dipartimento di Fisica del Politecnico di Milano, I-20133 Milano, Italy*
[3]*INRIM, Istituto Nazionale di Ricerca Metrologica, I-10135 Torino, Italy*

(Received 22 April 2013; published 8 August 2013)

We report on a new implementation of Doppler broadening thermometry based on precision absorption spectroscopy by means of a pair of offset-frequency locked extended-cavity diode lasers at 1.39 $\mu$m. The method consists in the highly accurate observation of the shape of the $4_{4,1} \rightarrow 4_{4,0}$ line of the $H_2{}^{18}O$ $\nu_1 + \nu_3$ band, in a water vapor sample at thermodynamic equilibrium. A sophisticated and extremely refined spectral analysis procedure is adopted for the retrieval of the Doppler width as a function of the gas pressure, taking into account the Dicke narrowing effect, the speed dependence of relaxation rates, and the physical correlation between velocity-changing and dephasing collisions. A spectroscopic determination of the Boltzmann constant with a combined (type *A* and type *B*) uncertainty of 24 parts over $10^6$ is reported. This is the best result obtained so far by means of an optical method. Our determination is in agreement with the recommended CODATA value.

DOI: 10.1103/PhysRevLett.111.060803 PACS numbers: 06.20.Jr, 33.70.Jg, 42.62.Fi

The Boltzmann constant ($k_B$) is presently the subject of considerable effort aimed at accurately measuring its value as the basis for a possible redefinition of the unit kelvin. The most accurate way to access the value of $k_B$ is from measurements of the speed of sound in a noble gas inside an acoustic resonator [1]. After over 40 years of research and technical developments, acoustic gas thermometry has recently provided a $k_B$ determination with a relative uncertainty of 0.71 parts over $10^6$ [2]. Another approach, known as dielectric constant gas thermometry and based upon the Clausius-Mossotti equation, has led to a value with a combined uncertainty of $9.2 \times 10^{-6}$ [3]. Other upcoming primary thermometry techniques are currently at the stage of further development and optimization. Among them, the newest and most promising one is known as Doppler broadening thermometry (DBT). Based upon precision laser spectroscopy in the linear regime of interaction, DBT consists in retrieving the Doppler width from the highly accurate observation of the profile corresponding to a given atomic or molecular line in a gas sample at the thermodynamic equilibrium [4]. Ammonia was the first thermometric substance employed in a DBT experiment, its spectrum being probed by a frequency-stabilized $CO_2$ laser at 10.34 $\mu$m [5]. In a subsequent implementation, an extended-cavity diode laser (ECDL) at 2 $\mu$m was used to interrogate a vibration-rotation transition of $CO_2$ [6]. In these first experiments, spectral analysis was performed by using either a Gaussian or a Voigt profile. In the last few years, with the ambitious goal of approaching the target accuracy of 1 part per million (ppm), technical improvements of the experimental setups have been accompanied by a more and more refined interpolation of the absorption line shapes, also involving other molecular targets, such as oxygen, acetylene, and water [7–9]. Particularly, great attention has been paid to the role of speed dependence of relaxation rates [10,11]. In spite of that, the most accurate spectroscopic determination of $k_B$ still exhibits a relatively large uncertainty, namely 144 ppm, with a statistical contribution of 6.4 ppm, resulting from the analysis of over 7000 spectra [12].

In this Letter, we report on the outcomes of a radically new DBT experiment, based upon a pair of offset-frequency locked extended-cavity diode lasers at 1.39 $\mu$m to probe the $4_{4,1} \rightarrow 4_{4,0}$ line of the $H_2{}^{18}O$ $\nu_1 + \nu_3$ band. The active and highly precise control of the emission frequency of the probe laser, as compared to an ultrastable reference laser, allowed us to build an absolute and reproducible frequency scale underneath the absorption spectra, thus satisfying one of the main requirements for a low-uncertainty DBT implementation. As far as the spectral analysis is concerned, an important element of novelty of the present work is the fact that speed-dependent and Dicke narrowing effects have been jointly considered for the aims of a spectroscopic determination of $k_B$. In fact, we adopted the so-called partially correlated speed-dependent hard-collision (PCSDHC) model to process hundreds of spectra, thus, providing a new value for $k_B$ with a combined uncertainty of 24 parts over $10^6$.

The experimental apparatus, depicted in Fig. 1, consists of an extended-cavity diode laser, an optoelectronic system for frequency stabilization and control, an intensity-control feedback loop, a sophisticated isothermal cell, and a detection chain. A highly effective stabilization and synchronization of the laser frequency is performed by using the

 

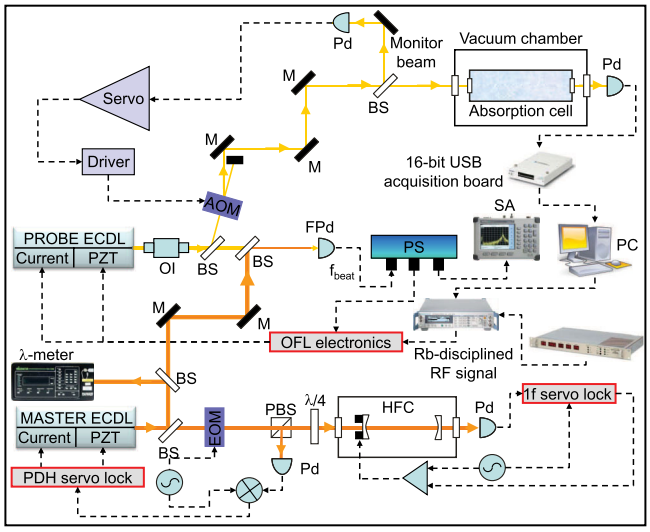


FIG. 1 (color online). Schematic diagram of the dual-laser absorption spectrometer. OI, optical isolator; BS, beam splitter; AOM, acousto-optic modulator; EOM, electro-optic modulator; $f_{\mathrm{beat}}$, beat frequency; $\lambda/4$, quarter wave plate; M, mirror; PBS, polarizing beam splitter; Pd, photodiode; FPd, fast photodiode; PS, radio frequency power-splitter; OFL, offset-frequency locking; HFC, high-finesse cavity; SA, spectrum analyzer; PC, personal computer.

technique of offset-frequency locking, in which the probe laser is forced to maintain a precise frequency-offset from a reference laser [13]. This offset is provided by a radio-frequency (rf) synthesizer, which in turn is phase locked to an ultrastable Rb oscillator. The reference (master) laser presents a subkilohertz absolute stabilization of its central frequency, being locked to an ultranarrow saturated absorption signal, resulting from the nonlinear interaction that occurs inside a high-finesse optical resonator, in coincidence with the $4_{4,0} \rightarrow 4_{4,1}$ line of the $H_2{}^{18}O$ $\nu_1 + \nu_3$ band. Specifically, the laser frequency was locked to the cavity by means of the Pound-Drever-Hall technique, while the cavity-mode frequency was actively stabilized against the center of the Lamb dip by using a dispersive signal, as provided by the first-derivative detection method, after dithering the cavity resonance by means of a sinusoidal signal at 2 kHz [14]. The emission wavelength of the reference laser is constantly measured by means of a seven-digit wave meter. Hence, the beat note between reference and probe lasers is first detected by means of a fast photodiode, properly amplified, scaled in frequency, and subsequently compared with the rf signal, so as to produce an error signal driving a double-servo system, which in turn acts on the diode injection current and on the extended-cavity length of the probe laser. By tuning the rf frequency, it is possible to perform continuous, highly linear and highly accurate frequency scans of the probe laser around a given center frequency.

Amplitude variation in the background baseline, which usually leads to one of the most subtle sources of systematic deviations, is essentially removed by implementing an intensity control feedback loop, which effectively compensates for any power variation associated to a laser frequency scan, as well as for the periodic modulation of the power arising from spurious etalon effects. Intensity stabilization at the level of $10^{-4}$ is achieved by using an acousto-optic modulator as an external actuator to continuously control the amount of laser power that is deflected from the primary beam to the first diffracted order, which is used for the DBT experiment.

Laser-gas interaction takes place inside a temperature-stabilized cylindrical cell, housed in a vacuum chamber. Equipped with a pair of antireflection-coated BK7 windows, the isothermal cell is 15 cm long and is actively kept at the temperature of the triple point of water, with stability in time and uniformity at the level of 0.15 mK, as extensively described elsewhere [15]. Temperature measurements are performed by using a pair of capsule-type standard platinum resistance thermometers, calibrated at the triple point of water, and an automatic resistance bridge. As a result, the overall uncertainty in temperature measurements amounts to about 0.3 mK.

A 97% enriched $^{18}O$ water sample (with a nominal purity better than 99.9%) is used to fill the gas cell at a variable pressure, as measured by means of an absolute pressure gauge. After four passes through the isothermal cell, the transmitted beam is probed by a ultralow-noise preamplified InGaAs photodiode, whose voltage signal is digitized by a data acquisition board with a 16-bit resolution and a sampling rate of $1 \times 10^6$ samples. The possible nonlinearity of the detection chain was estimated to be well below the noise level. A LABVIEW code allowed us to control the whole setup, to perform step-by-step frequency scans and to acquire, for each step, the transmitted signal.

A major effort in our work was devoted to line shape modeling, which is far from being trivial for self-colliding $H_2O$ molecules. In fact, deviations from the Voigt model are clearly observed even in the case of pure $H_2O$ samples at relatively small pressures [10]. In this respect, the molecular confinement alone is revealed to be unable to explain entirely these departures, while the speed dependence of pressure-induced broadening and shifting must be considered [9,10]. In a recent theoretical study, the partially correlated speed-dependent Keilson-Storer (PCSDKS) model has been proposed to describe $H_2O$ line shapes [16]. Comparisons between simulated spectra and measurements have shown excellent agreements, thus demonstrating the existence of a partial correlation between velocity-changing collisions and rotational-state-changing collisions, as described by a correlation parameter, $\eta$, which was found to be 0.2 [17]. Because of its complexity and large computational cost, the PCSDKS model could not be implemented into a fitting procedure. Instead, it was used as a benchmark

to test the validity of simplified semiclassical approaches. Among them, the PCSDHC model was revealed to be the most appropriate for describing our physical situation [17]. In the present work, we successfully employed this model, thus, performing nonlinear least-square fits of hundreds of spectra, acquired in the pressure range between 200 and 500 Pa. In particular, we adopted the following form [18,19]:

$$\mathrm{PCSDHC}(\omega) = \frac{1}{\pi}\,\mathrm{Re}\left[\frac{G(\omega)}{1-\mathrm{H}(\omega)}\right], \tag{1}$$

$$G(\omega) = \int_{-\infty}^{+\infty} d\vec{v}\,\frac{W_M(\vec{v})}{\beta_V(v)+\beta_{VD}(v)+\Gamma_D(v)-i[\omega-\omega_L-\Delta_D(v)-\vec{k}\cdot\vec{v}]}, \tag{2}$$

$$H(\omega) = \int_{-\infty}^{+\infty} d\vec{v}\,\frac{W_M(\vec{v})[\beta_V(v)+\beta_{VD}(v)-\Gamma_{VD}(v)-i\Delta_{VD}(v)]}{\beta_V(v)+\beta_{VD}(v)+\Gamma_D(v)-i[\omega-\omega_L-\Delta_D(v)-\vec{k}\cdot\vec{v}]}. \tag{3}$$

Here, Re means real part, $W_M(\vec{v})$ is the Maxwell-Boltzmann velocity distribution, $v = |\vec{v}|$ is the absorber speed, $\omega$ is the angular frequency, $\omega_L$ is the collisionless rest frequency of the transition, and $k = \omega_L/c$, being $c$ the vacuum speed of light. The total collision rate, collisional width, and shift, are, respectively, given by $\beta = \beta_V + \beta_{VD}$, $\Gamma = \Gamma_D + \Gamma_{VD}$, and $\Delta = \Delta_D + \Delta_{VD}$, where the subscript $V$ refers to purely velocity-changing collisions, $D$ purely dephasing collisions, and $VD$ simultaneous velocity-changing and dephasing collisions. It is possible to write $\beta_{VD} = \eta\beta$, $\Gamma_{VD} = \eta\Gamma$, and $\Delta_{VD} = \eta\Delta$. Speed dependence is assumed to be identical for $\beta$ and $\Gamma$, while it is ignored for $\Delta$, since we did not observe any asymmetry in the experimental profiles, at any pressure. It is expressed in terms of a confluent hypergeometric function, $M(a;b;x)$, which results from the application of the Berman-Pickett formalism [20,21]. In particular, the collisional width is given by

$$\Gamma(v) = \frac{\Gamma_0}{2^{m/2}} M\left(\frac{-m}{2};\frac{3}{2};-\left(\frac{v}{v_0}\right)^2\right), \tag{4}$$

$\Gamma_0 = \langle\Gamma(v)\rangle$ being the average collisional width over molecular speeds and $v_0$ the most probable speed. The quantity $m$ is given by $(q-3)/(q-1)$, where $q$ is the exponent determining the collision interaction potential, which is assumed of the form $V(R) \sim R^{-q}$, $R$ being the intermolecular distance [21].

Figure 2 shows a typical transmission spectrum for the $H_2{}^{18}O$ $4_{4,1} \rightarrow 4_{4,0}$ line at ~270 Pa, along with fit residuals computed as deviations between theory and experiment. Laser scans were 3.1 GHz wide and resulted from 3100 steps of 1 MHz each, with a step-by-step acquisition time of 100 ms. This and all the other spectra were fitted to the function $P(\nu) = (P_0 + P_1\nu)\exp[-Ag(\nu-\nu_0)]$, where $\nu$ is the frequency detuning from the reference laser, $\nu_0$ is the central frequency, $A$ is the integrated absorbance, $g(\nu-\nu_0)$ is the PCSDHC profile, while the parameters $P_0$ and $P_1$ account for a possible residual variation of the incident power. The fitting procedure was implemented under the MATLAB environment, using the trust region optimization algorithm. Free parameters were $\nu_0$, $A$, $P_0$, $P_1$, $\Gamma_0$, $\Delta$, $\beta_0$ ($\beta_0$ being the average collision frequency over molecular speeds) and $\Delta\nu_D$, which is the Doppler width (HWHM). This latter is rather hidden in Eq. (1), while it appears more clearly after the angular integration, with the polar axis along the wave vector [19]. The parameters $\eta$ and $q$ were fixed at 0.2 and 5.017, respectively. If, for the $\eta$ value, we could exploit the outcomes of Ref. [17], the choice of the $q$ value required a specific study. It should be noted that if we repeat the fit of Fig. 2 with a Gaussian or a Voigt profile, the resulting Doppler width differs from the expected value by +13 and −5 MHz, respectively.

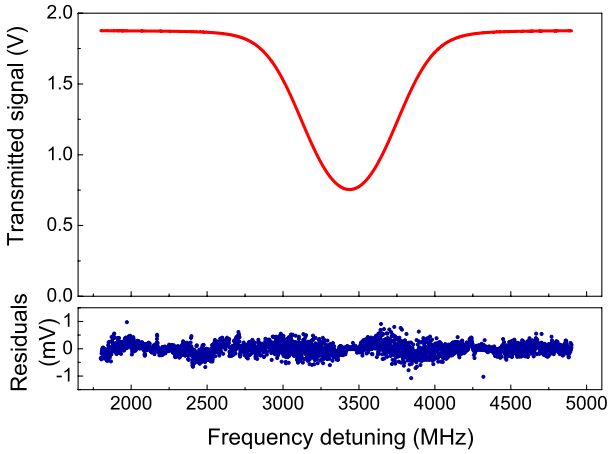


FIG. 2 (color online). Experimental $H_2{}^{18}O$ spectrum near $\lambda = 1.39$ $\mu$m, at a pressure of about 2 Torr and a temperature of 273.1550 K. The signal-to-noise ratio was measured to be ~10 000. Absolute residuals are also reported, resulting from the nonlinear least-squares fit to the PCSDHC profile. The root-mean-square value of the residuals amounts to about 200 $\mu$V, while the reduced $\chi^2$ value is 0.22. The same level of agreement between theory and experiment has been obtained in the whole pressure range.

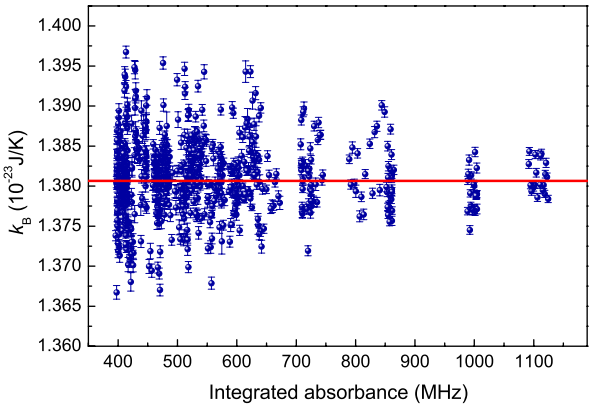


FIG. 3 (color online). Spectroscopic determination of the Boltzmann constant. The red line represents the current CODATA value, namely $1.380\,648\,8(13) \times 10^{-23}$ J/K. Error bars, corresponding to one standard deviation, are the internal errors resulting from the fitting procedure.

Once $\Delta\nu_D$ has been retrieved from a given spectrum, $k_B$ can be readily obtained by inverting the formula:

$$\Delta\nu_D = \frac{\nu_L}{c}\sqrt{2\ln 2\frac{k_B T}{M}}, \tag{5}$$

being $c$ the vacuum speed of the light, $\nu_L = \omega_L/(2\pi)$, $T$ the thermodynamic temperature, and $M$ the mass of the molecule. In Fig. 3, we report the measured $k_B$ values as a function of the integrated absorbance (which is proportional to the gas pressure), resulting from the analysis of 718 spectra. We note a growing fluctuation of the data points with decreasing pressures. This is caused by the decreasing signal-to-noise ratio and by the statistical correlation of $\Delta\nu_D$ with $\Gamma_0$, $A$, and $\beta_0$. To give an idea, the correlation coefficients amount to $-0.97$, $-0.88$, and $+0.89$, respectively, for the fit of Fig. 2. Extensive tests on simulated spectra have shown that the effect of these correlations is that of limiting the achievable reproducibility, rather than influencing the mean value over repeated determinations. The optimum $q$ value was identified only after repeatedly applying the fitting procedure to the whole set of spectra, looking for the situation of a zero slope in the weighted linear fit of the $k_B$ data versus the integrated absorbance. Each time a different value for the $q$ parameter was set. So doing, the zero slope was found for $q$ values in the interval given by $5.017 \pm 0.017$.

The weighted mean of the values of Fig. 3 amounts to $(1.380\,631 \pm 0.000\,022) \times 10^{-23}$ J/K, which gives a relative statistical uncertainty of about 16 ppm. Table I summarizes the complete uncertainty budget, which leads to a combined uncertainty of 24 ppm. This is a factor of 6 better than the best result obtained so far [12]. The main sources of systematic deviations are ascribed to the line shape model and to the frequency-modulation (FM) broadening effect. As for the line shape model, we calculated the variation of the weighted mean associated to the uncertainty on the $q$ value. Moreover, we found that a different choice for $\eta$ (between 0.1 and 0.5) had a negligible influence on the retrieved Doppler widths, while it strongly affected the $\beta_0$ value. As for FM broadening, we have shown that a modulation of the optical cavity length was necessary in order to build the absolute frequency reference. Unfortunately, this frequency dither was transferred from the reference to the probe laser, being the modulation frequency well within the bandwidth of the locking loop. As a result, a broadening of the emission width up to the level of 1 MHz (FWHM) was measured, with a consequent perturbation of the absorption profile. Such a broadening effect was accurately quantified by measuring, as a function of the dither amplitude, the width of the beat note between the locked probe laser and the nearest tooth of an erbium-doped fiber-laser comb. The analysis of numerically simulated spectra, in which a Voigt model was adopted for the emission profile of the probe laser, entering into the convolution with the line profile, allowed us to quantify the influence on the determination of $k_B$, which amounted to 10 ppm. It is worth noting that hyperfine structure (HFS) effects could be neglected, despite the fact that the selected transition is of the ortho type [22]. Similarly, we could completely ignore any effect due to a possible saturation of the line.

TABLE I. Uncertainty budget (in terms of relative contributions, corresponding to one standard deviation) for the spectroscopic determination of $k_B$.

| Contribution | Type $A$ | Type $B$ |
|---|---|---|
| Experimental reproducibility | $15.7 \times 10^{-6}$ | |
| Frequency scale uncertainty | | $2.6 \times 10^{-6}$ |
| Line-center frequency | | $0.278 \times 10^{-6}$ |
| Laser emission width and FM broadening | | $\sim 10 \times 10^{-6}$ |
| Saturation broadening | | Negligible |
| Detector nonlinearity | | Negligible |
| Spurious etalon effects | | Negligible |
| Cell's temperature | | $1.1 \times 10^{-6}$ |
| Hyperfine structure effects | | Negligible |
| Line shape model | | $14.9 \times 10^{-6}$ |
| Total uncertainty | $24 \times 10^{-6}$ | |

In conclusion, we have reported on a significant step forward towards the development of low-uncertainty DBT. This achievement was made possible by using the technique of offset-frequency locking and by adopting a very refined and reliable line shape model for the highly accurate retrieval of the Doppler width from a well isolated experimental profile. Characterized by a combined uncertainty of 24 parts over $10^6$, our $k_B$ value agrees with recent determinations resulting from more conventional methods [2,3]. A further reduction of the uncertainty can be pursued by increasing the number of spectra, possibly enlarging the pressure interval, by improving

the signal-to-noise ratio and by removing the dither on the reference laser. As for this latter upgrade, we are presently implementing the technique known as noise-immune cavity-enhanced optical heterodyne molecular spectroscopy for the highly sensitive detection of the sub-Doppler line. As for the line shape problem, we plan to use even more sophisticated profiles, in the near future. For instance, we intend to implement another version of the PCSDHC model, following the approach proposed in Ref. [23]. Moreover, the uncertainty associated to the line shape model will be significantly reduced once a global analysis approach will be developed to simultaneously fit a manifold of profiles across a given range of pressures, sharing a restricted number of unknown parameters, including $q$ and $\Delta\nu_D$. This approach would also reduce fluctuations resulting from statistical correlations among free parameters, as clearly demonstrated in Ref. [24]. On the basis of a first global analysis done on a restricted number of spectra ($<10$), we anticipate a reduction of the statistical uncertainty by a factor of $\sim$10, as compared to the outcomes of individual fits. We are also considering the exploration of other physical situations that could be much more accurately modeled, such as trace amounts of water in a bath of noble gas atoms, acting as hard spheres either much lighter or much heavier than the absorbing molecules.

Our results open new interesting perspectives towards the achievement of the target accuracy of 1 ppm in the spectroscopic determination of $k_B$. Hence, we expect to contribute to the new definition of unit kelvin, also providing a new powerful tool for the realization of the future thermodynamic temperature scale.

We gratefully acknowledge funding from EMRP through Project No. SIB01-REG3. The EMRP is jointly funded by the EMRP participating countries within EURAMET and the European Union.

*Corresponding author.
livio.gianfrani@unina2.it

[1] M. R. Moldover, J. P. M. Trusler, T. J. Edwards, J. B. Mehl, and R. S. Davis, Phys. Rev. Lett. **60**, 249 (1988).
[2] M. de Podesta, R. Underwood, G. Sutton, P. Morantz, P. Harris, D. F. Mark, F. M. Stuart, G. Vargha, and G. Machin, Metrologia **50**, 354 (2013).
[3] B. Fellmuth, J. Fischer, C. Gaiser, O. Jusko, T. Priruenrom, W. Sabuga, and T. Zandt, Metrologia **48**, 382 (2011).
[4] C. J. Bordé, Metrologia **39**, 435 (2002).
[5] C. Daussy, M. Guinet, A. Amy-Klein, K. Djerroud, Y. Hermier, S. Briaudeau, C. J. Bordé, and C. Chardonnet, Phys. Rev. Lett. **98**, 250801 (2007).
[6] G. Casa, A. Castrillo, G. Galzerano, R. Wehr, A. Merlone, D. Di Serafino, P. Laporta, and L. Gianfrani, Phys. Rev. Lett. **100**, 200801 (2008).
[7] A. Cygan, D. Lisak, R. S. Trawiński, and R. Ciuryło, Phys. Rev. A **82**, 032515 (2010).
[8] K. M. Yamada, A. Onae, F.-L. Hong, H. Inaba, and T. Shimizu, C.R. Phys. **10**, 907 (2009).
[9] M. D. De Vizia, L. Moretti, A. Castrillo, E. Fasci, and L. Gianfrani, Mol. Phys. **109**, 2291 (2011).
[10] M. D. De Vizia, F. Rohart, A. Castrillo, E. Fasci, L. Moretti, and L. Gianfrani, Phys. Rev. A **83**, 052506 (2011).
[11] M. Triki, C. Lemarchand, B. Darquié, P. L. T. Sow, V. Roncin, C. Chardonnet, and C. Daussy, Phys. Rev. A **85**, 062510 (2012).
[12] C. Lemarchand, M. Triki, B. Darquié, C. J. Bordé, C. Chardonnet, and C. Daussy, New J. Phys. **13**, 073028 (2011).
[13] A. Castrillo, E. Fasci, G. Galzerano, G. Casa, P. Laporta, and L. Gianfrani, Opt. Express **18**, 21851 (2010).
[14] G. Galzerano, E. Fasci, A. Castrillo, N. Coluccelli, L. Gianfrani, and P. Laporta, Opt. Lett. **34**, 3107 (2009).
[15] A. Merlone, F. Moro, A. Castrillo, and L. Gianfrani, Int. J. Thermophys. **31**, 1360 (2010).
[16] N. H. Ngo, H. Tran, and R. R. Gamache, J. Chem. Phys. **136**, 154310 (2012).
[17] H. Tran, N. H. Ngo, J.-M. Hartmann, R. R. Gamache, D. Mondelain, S. Kassi, A. Campargue, L. Gianfrani, A. Castrillo, E. Fasci, and F. Rohart, J. Chem. Phys. **138**, 034302 (2013).
[18] A. S. Pine, J. Chem. Phys. **101**, 3444 (1994).
[19] A. Pine, J. Quant. Spectrosc. Radiat. Transfer **62**, 397 (1999).
[20] P. R. Berman, J. Quant. Spectrosc. Radiat. Transfer **12**, 1331 (1972).
[21] H. M. Pickett, J. Chem. Phys. **73**, 6090 (1980).
[22] C. Puzzarini, G. Cazzoli, M. E. Harding, J. Vázquez, and J. Gauss, J. Chem. Phys. **131**, 234304 (2009).
[23] P. Wcislo and R. Ciurylo, J. Quant. Spectrosc. Radiat. Transfer **120**, 36 (2013).
[24] A. Pine and T. Gabard, J. Quant. Spectrosc. Radiat. Transfer **66**, 69 (2000).